DOI:
10.1016/j.nucmedbio.2018.10.004

Document Version
Peer reviewed version

Unexpected decrease in in vivo binding of [3H]QNB in the mouse cerebral cortex in the developing brain - a comparison with [11C]NMPB

Osamu Inoue, Toshiyuki Sato, Kaoru Kobayashi, Antony Gee, Miho Shukuri, Ming-Rong Zhang

PII: S0969-8051(18)30273-7
DOI: doi:10.1016/j.nucmedbio.2018.10.004
Reference: NMB 8042

To appear in: *Nuclear Medicine and Biology*

Received date: 30 August 2018
Revised date: 3 October 2018
Accepted date: 11 October 2018

Please cite this article as: Osamu Inoue, Toshiyuki Sato, Kaoru Kobayashi, Antony Gee, Miho Shukuri, Ming-Rong Zhang , Unexpected decrease in in vivo binding of [3H]QNB in the mouse cerebral cortex in the developing brain - a comparison with [11C]NMPB. Nmb (2018), doi:10.1016/j.nucmedbio.2018.10.004

Unexpected decrease in *in vivo* binding of [^{3}H]QNB in the mouse cerebral cortex in the developing brain - A comparison with [^{11}C]NMPB

Abbreviated title: [^{3}H]QNB binding in the developing mouse brain

Osamu Inoue [a,*], Toshiyuki Sato [a], Kaoru Kobayashi [a], Antony Gee [b], Miho Shukuri [c], Ming-Rong Zhang [a,*]

[a] Department of Radiopharmaceuticals Development, National Institute of Radiological Sciences, National Institutes for Quantum and Radiological Science and Technology, Chiba 263-8555, Japan.

[b] School of Biomedical Engineering and Imaging Sciences, King's College London, 4th Floor Lambeth Wing, St. Thomas' Hospital, London, SE1 7EH, UK.

[c] Laboratory of Physical Chemistry, Showa Pharmaceutical University, Machida 194-8543, Japan.

* Corresponding Author

1. Osamu Inoue, Department of Radiopharmaceuticals Development, National Institute

of Radiological Sciences, National Institutes for Quantum and Radiological Science and Technology, 4-9-1 Anagawa, Inage-ku, Chiba 263-8555, Japan.

Email: oinoue@asahinet.jp.

2. Ming-Rong Zhang, Department of Radiopharmaceuticals Development, National Institute of Radiological Sciences, National Institutes for Quantum and Radiological Science and Technology, 4-9-1 Anagawa, Inage-ku, Chiba 263-8555, Japan.

E-mail: zhang.ming-rong@qst.go.jp.

Key Words: [^{3}H]QNB, [^{11}C]NMPB, Development, mouse, brain, diffusion boundary

ABSTRACT

Introduction

Significant discrepancies between *in vitro* and *in vivo* binding of the muscarinic receptor ligand - ^{3}H-labeled Quinuclidinyl Benzylate (QNB) - have been well documented. Discernable *in vivo* cerebellar [^{3}H]QNB binding has been observed in mouse brain, despite the maximum number of binding sites (Bmax) being low. In order to understand this unique *in vivo* binding phenomenon, the binding of two muscarinic receptor ligands -[^{3}H]QNB and *N*-[^{11}C]methylpiperidyl Benzylate ([^{11}C]NMPB) - were compared *in vivo and in vitro* in 3- and 8-week-old mice.

Method

In vitro binding parameters of [^{3}H]QNB were determined using brain homogenates. The time course of radioactivity concentration (TACs) in the cerebral cortex and cerebellum were measured following injection of [^{3}H]QNB and [^{11}C]NMPB with or without 3 mg/kg of carrier QNB in 3- and 8 week old mice using a dual tracer administration technique. A graphical method was employed for the quantitative analysis of *in vivo* binding of

these radioligands.

Results

In vitro, the available number of binding sites for cerebral cortical muscarinic receptors increased by 17% during the developmental period studied. Paradoxically, *in vivo*, we observed a decrease of [^{3}H]QNB binding in the cerebral cortex, whilst [^{11}C]NMPB binding was markedly increased. *In vivo* saturation analysis of [^{3}H]QNB in 3-week-old mice revealed an apparent positive cooperativity of binding in the cerebral cortex.

Conclusions

Our results support the hypothesis that microenvironmental factors proximal to muscarinic receptors cause a local decrease in the cortical free-ligand concentration of [^{3}H]QNB and that this 'ligand barrier' is modulated during brain development.

Advances in Knowledge

The present study demonstrates that the combined use of radiolabeled QNB and NMPB has the potential to reveal the important effects of receptor microenvironmental factors on receptor function in the living brain.

1. Introduction

Muscarinic receptors play essential roles in both the central nervous system (CNS) [1-3] and peripheral tissues [4, 5]. They have been pharmacologically classified into three subclasses: M1, M2, and M3 [6]. M1 receptors are predominantly expressed in the striatum, cerebral cortex, and hippocampus, while M2 receptors are mainly distributed in the cerebellum and heart [7, 8].

In vitro binding studies of muscarinic receptors have employed labeled Quinuclidinyl Benzylate (QNB) and *N*-methylpiperidyl Benzylate (NMPB) as non-selective radioligands [9-16]. NMPB's *in vivo* binding mirrors its known *in vitro* distribution with characteristically low specific binding in the cerebellum, both *in vivo* and *in vitro* [16,18]. However, a conflicting *in vivo* cf. *in vitro* binding profile has been reported for [^{3}H]QNB in the intact brain [17, 18]: the specific binding of [^{3}H]QNB in the cerebellum of living mice or rats is considerably higher than that measured *in vitro*. In

addition, *in vivo* saturation experiments on [^{3}H]QNB binding show non-linear (positive cooperativity) binding in the cortex and linear saturable binding in the cerebellum [18] The aim of the study was to measure changes in binding parameters of [^{3}H]QNB and [^{11}C]NMPB during the CNS development process. 3 week old mice were selected as the juvenile group, purely on the basis of practicalilities of i.v. cannulation. Mice bellow 3 weeks of age were excluded because of the size of veins and difficulties in performing i.v. injections in these smaller animals. Eight weeks old mice were chosen as adult group. As the *in vivo* dissociation rate of [^{3}H]QNB in the brain (0-60 min) is negligible, specific binding is dependent upon the forward-rate constant k_3. The k_3 includes three components: free ligand concentration [F], the bimolecular rate constant (kon) and available binding sites (Bmax). *In vivo* saturation experiments have shown that Bmax in the cerebellum is 15-fold lower than that in the cerebral cortex [18]. However, the present study observed a significant, unexpected decrease in the *in vivo* binding of [^{3}H]QNB in the cerebral cortex during the 3-8 week development period.

We speculate that the ligand-concentration dependent modulation of the free ligand concentration proximal to the receptors in the cerebral cortex is due to a diffusion boundary – a concept initially introduced by Perry et al. [19]. Several lines of evidence strongly indicate that membrane fluidity and lipid components in membranes modulate

receptor binding and receptor function [20-25]. To the best of our knowledge, this study is the first to provide evidence for a modulatory role of the diffusion boundary upon receptor function in the developing brain.

2. Materials and methods

2.1. Labeled compounds and chemicals

(R)-[^{3}H]QNB (molar activity: 1.44 GBq/μmol) was provided by New England Nuclear Research Product. *(R)*-QNB was provided by Research Biochemicals International. [^{11}C]NMPB (molar activity: 55.5 GBq/μmol) was synthesized using [^{11}C]methyl iodide according to a previously reported method [26]. (-)-Scopolamine hydrochloride was obtained from Sigma-Aldrich.

2.2. Animals

Male ddY mice were provided by Japan SLC and housed under a 12—hour light cycle with free access to food and water. All animal experiments were approved by the Experimental Animal Committee of the National Institute of Radiological Sciences (Chiba, Japan).

2.3. In vitro homogenate [^{3}H]QNB binding of the cerebral cortex and cerebellum of 3- and 8-weeks-old mice

Mice (3 and 8 weeks old; the body weights were 12 g and 33 g, respectively) were decapitated under diethyl ether anesthesia, and their brains were rapidly removed. Homogenates of the cerebral cortex and cerebellum were prepared as 0.05 M Na-K phosphate buffer solutions (1 mg/mL: cerebral cortex; 2 or 5 mg/mL: cerebellum). [^{3}H]QNB was dissolved in 0.05 M Na-K phosphate buffer solution (from 100 pM to 2000 pM). Each homogenate solution was incubated with 1 mL of [^{3}H]QNB at 37°C for 30 minutes. After incubation, the B/F separation was made using glass filters (Whatmann, CF/C Filter). The incubation tubes were washed twice with ice-cold buffer, and the glass filters were washed five times with ice-cold water. The filters were transferred into scintillation vials, and 10 mL of liquid scintillator (Packard, Hionic Flow) was added. Radioactivity in each vial was determined by a liquid-scintillation counter (Aloka, LSC-5100), and the non-specific binding (NSB) was determined using 1 μM of scopolamine. The specific binding was determined by subtraction of NSB from total radioactivity in each ligand concentration. The estimation of KD and Bmax values was performed by using the Scachard Plot.

2.4. Dual tracer protocol

[^{3}H]QNB (0.2 mL; 74 KBq) and [^{11}C]NMPB (0.2 mL; 3.5MBq) were intravenously injected into 3- and 8-week-old mice, which were subsequently decapitated under diethyl ether at 1, 5, 10, 20, 30, 45, and 60 minutes post-injection. The brains were quickly removed, and dissected into the cerebral cortex and cerebellum. After weighing the specimens, the radioactivity of ^{11}C of each sample was measured via a gamma well-counter (Packard 5230). After the decay of ^{11}C was determined, each sample was dissolved using a tissue solubilizer (Packard; Soluene 350). The radioactivity of each sample was determined by a liquid scintillation counter (Beckman; LS6800).

The *in vivo* time course of radioactivity concentration (TAC) was determined in the plasma and brains of 3- and 8-week-old mice. Non-specific binding (NSB) was ascertained by measuring the TAC in each region following the intravenous injection of [^{3}H]QNB and [^{11}C]NMPB together with 3 mg/kg of the carrier QNB.

2.5. Kinetic analysis of in vivo [^{3}H]QNB and [^{11}C]NMPB binding in the cerebral cortex and cerebellum

The graphical method (the Patlak plot) [27] was employed for the quantitative analysis of *in vivo* [^{3}H]QNB and [^{11}C]NMPB binding in the cerebral cortex and

cerebellum. The TACs of [^{3}H]QNB or [^{11}C]NMPB with 3 mg/kg of carrier QNB in the cerebellum were used to estimate the free-ligand concentration in the brain and as input functions for the kinetic analysis. The binding parameter, k_3, of [^{3}H]QNB and [^{11}C]NMPB in the cerebral cortex and cerebellum of 3-and 8-weeks-old mice were estimated.

2.6. In vivo saturation study of [^{3}H]QNB binding in the cerebral cortex and cerebellum of 3-weeks old mice

Mice (n = 3) were intravenously injected with [^{3}H]QNB together with different doses of non-radioactive QNB, ranging from 3 μg/kg to 3000 μg/kg, and were sacrificed by decapitation under ethyl ether anesthesia 60 min after the injection. Radioactivity in the cerebral cortex and cerebellum was measured as described above. Specific binding was calculated by subtracting the radioactivity concentration in the cerebellum (co-injected with 3000 μg/kg of [^{3}H]QNB) from the corresponding radioactivity concentration in each region.

2.7. Statistical analysis

Student's-t test was used for the statistical analysis.

3. Results

The results of the *in vitro* binding in the cerebral cortex and cerebellum in 3- and 8-weeks-old mice are shown in Table 1. In the cerebral cortex, [^{3}H]QNB bound to a single binding site. Bmax in the cerebral cortex increased during the development period with no significant changes in affinity. In the cerebellum, no significant difference of binding parameters were observed.

The time course of [^{3}H]QNB and [^{11}C]NMPB radioactivity concentrations (TAC) in the cerebral cortex and cerebellum of 3-weeks-old mice (with or without the 3 mg/kg of carrier), are summarized in Tables 2, and 3. TACs for 8-week-old mice are shown in Tables 4 and 5. In 3-week-old mice, radioactivity was highly retained in the brain when [^{3}H]QNB was injected at tracer doses. However, when [^{3}H]QNB was injected together with the 3 mg/kg of the carrier, radioactivity concentrations in the brain decreased rapidly over time. A similar result was found in 8-week-old mice. The TACs for [^{11}C]NMPB binding in 3- and 8-week-old mice, with or without carrier QNB, are shown in Tables 3 and 5. When [^{11}C]NMPB was injected at tracer levels, higher radioactivity concentrations were observed in the cerebral cortex of both 3- and 8-week-old mice relative to radioactivity concentrations of [^{3}H]QNB. When the 3 mg/kg of carrier QNB was injected together with [^{11}C]NMPB, a rapid tracer washout was observed in the

brains of 3- and 8-week-old mice. The Patlak plots for [^{3}H]QNB and [^{11}C]NMPB binding in the cerebral cortex and cerebellum of 3- and 8-weeks-old mice are shown in Figures 1 and 2. Linear slopes were observed for both [^{3}H]QNB and [^{11}C]NMPB binding in the cerebral cortex of 3- and 8-weeks-old mice. The slope of the straight line for [^{3}H]QNB binding in 8-week-old mice was significantly shallower than that in 3-weeks-old mice, whereas that of [^{11}C]NMPB in the cerebral cortex of 8-week-old mice was steeper than that in 3-weeks-old mice. In the cerebellum, no significant difference in the slope of the line for [^{3}H]QNB was observed between 3- and 8-week-old mice. The estimated k_3 values for [^{11}C]NMPB and [^{3}H]QNB binding in the cerebral cortex and cerebellum are shown in Figures 1 and 2.

The results of the *in vivo* [^{3}H]QNB saturation experiments in 3-week-old mice are shown in Table 6 and Figure 3. Positive cooperativity of *in vivo* binding in the cerebral cortex was observed, while a simple competitive inhibition was found in the cerebellum.

4. Discussion

The *in vitro* Bmax of muscarinic receptors in the cerebral cortex significantly increased during the CNS development process, while the affinity of [^{3}H]QNB remained unchanged. In the cerebellum, no significant changes in the binding parameters were

seen. The M1 subtype of the muscarinic receptors is known to be highly expressed in the cerebral cortex and striatum, while M2 receptors appear to be the predominant subtype expressed in the cerebellum and heart [7, 8]. Our *in vitro* binding data therefore suggests that the M1-receptor expression in the cerebral cortex increases over the 3 to 8 weeks period of development. These data are consistent with those of a previous report, which found that, *in vitro*, the amount of QNB bound per mg membrane protein increased in whole-mouse-brain preparations from 14 to 42 days of age with no change in ligand affinity [28].

The most important finding of this study is that the *in vivo* binding of [^{3}H]QNB in the cerebral cortex of 8-week-old mice significantly decreases relative to that of 3-week-old mice, despite an increase in Bmax exhibited by the older mice. The kinetic analysis performed with the Patlak plot showed a significant reduction in [^{3}H]QNB binding (k_3) in the cerebral cortex from 3 to 8 weeks of age (Figure 1). However, a remarkable increase in [^{11}C]NMPB binding in this region was observed in 8-weeks-old mice. As shown in Figures 1 and 2, the slope of [^{3}H]QNB binding in the cerebral cortex of 8-week-old mice was less than 20% of that of the 3-week-old mice, while the slope for [^{11}C]NMPB binding in this region was increased in 8-week-old mice relative to the 3-week-old mice. On the other hand, the gradient of the slope for [^{3}H]QNB binding in

the cerebellum was not significantly different during the development period studied. The slope of the regression line, in this case, reflects k_3 of a two-compartment model and includes [F], kon, and Bmax. As previously reported, the *in vivo* binding of [^{11}C]NMPB parallels the distribution of muscarinic receptors in the brain, which suggested that NMPB was a non-subtype selective ligand both *in vitro* and *in vivo*.[16, 18]. Therefore, an increase in the binding potential of [^{11}C]NMPB in 8-week-old mice may relate to an increase in the Bmax in the developing brain. A significant decrease in cerebral cortical [^{3}H]QNB binding during the studied development period was an unexpected finding. Since the Bmax in the cerebral cortex was higher in 8-week-old mice, the reduction of the Patlak slope can be attributed to a decrease in either [F] or kon in the cerebral cortex. A difference in the radiotracer delivery from the plasma to the brain seems unlikely, because the TACs in the cerebral cortex good BBB permeability for both radioligands under carrier added conditions. Thus, the current observations may be accounted for by a decrease of either [F] or kon for [^{3}H]QNB in the cerebral cortex in the developing brain. [3H]QNB was well known non subtype selective ligand with high affinity(KD: 136 pM for rat cerebral and cerebellar synaptosomes)[29]. It has been well documented that Gilter et al. proposed that [^{3}H]QNB is an M2 selective ligand under *in vivo* conditions [17, 32], despite its being a non-subtype selective radioligand *in vitro*

[29]. Although the hypothesis that high accumulation of [^{3}H]QNB in the cerebellum (M2-subtype rich region) could be due to differences in the *in vivo* and *in vitro* subtype-selectivity of [^{3}H]-QNB, further evidence is required to test this possible explaination. Several brain permeable subtype-selective ligands are currently available. Bakker et al developed ^{123}I-iododexetimide as a M1 selective SPECT ligand [30]. [^{18}F]FP-TZTPI was evaluated as a M2 selective PET probe in subtype knockout mouse [31]. These subtype-selective ligands might be of value to verify the validity of the above hypothesis. The latter hypothesis, however, is not able to explain the current observation that *in vivo* binding of [^{3}H]QNB in the cerebral cortex is decreased during the development period, since the cerebral cortex is an M1-subtype rich region [7], The reason for selective changes in the kon of [^{3}H]QNB in the cerebral cortex during development is thus far unexplained. We, however, postulate that significant reductions in the free-ligand concentration surrounding the muscarinic receptor itself occur during the 3 to 8 weeks development period in mice. It is speculated that diffusion barriers cause this effect and that the heterogeneity of the microenvironment surrounding receptors plays a critical role in modulating effective free-ligand concentrations *in vivo*. Perry et al. introduced the concept of the diffusion boundary to explain the long-term retention of opioid antagonists in the intact brain [19]: the model posits that the

receptor micro-compartment consists of a population of binding sites next to a diffusion boundary, which restricts ligand diffusion away from the receptor. Interestingly, this diffusion boundary phenomenon disappears when brain tissue is homogenized [33], suggesting that the diffusion boundary may only be manifest *in vivo*. We expand the concept of the diffusion boundary by suggesting that the free-ligand concentration in a micro-compartment might be altered by microenvironments surrounding the receptors. These unknown barriers for [^{3}H]QNB binding either increase or change during the 3 to 8 week development process, although it is unclear whether such barriers are related to the interfacial effect we have previously proposed [34]. Providing further support for our hypothesis, the present experiment on *in vivo* [^{3}H]QNB binding in the brains of 3-week-old mice revealed positive cooperativity of binding in the cerebral cortex but not in the cerebellum (Figure 3).

Several lines of evidence indicate that alterations in membrane fluidity (and lipid membrane composition) affect receptor binding and function in the CNS [20-25]. Inactivation of muscarinic receptors in synaptic membranes by free fatty acids has been reported [20]. Dietary choline intake significantly increases the *in vivo* binding of [^{3}H]Ro15-1788 in all regions of the mouse brain [21]. Changes in striatal dopamine and acetylcholine receptors are induced by the chronic administration of cytidine

5'-diphosphocholine to aged mice [22]. The affinity of muscarinic receptors to antagonists is modulated by the lipid environment [23]. Lipid peroxidation causes changes in membrane fluidity as well as muscarinic receptor binding in the rat cerebral cortex [24]. In addition, lipid fluidity modulates the binding of serotonin to mouse brain membranes [25]. Taken together, these reports strongly suggest that lipid composition plays an essential role in ligand-receptor interactions, both *in vitro* and *in vivo*. To the best of our knowledge, there are no reports concerning the changes in lipid composition in the developing brain. Such alterations in lipid composition in the brain may, however, relate to changes in the diffusion barrier, the existence of which is supported by our measurements of [^{3}H]QNB binding in the cerebral cortex.

The reason for a barrier in the cerebral cortex and not in the cerebellum is unknown: however, it may be related to the high density of muscarinic receptors in this region. In fact, *in vivo* binding of [^{3}H]QNB in other receptor-rich areas, such as the striatum, also decreases at 8 weeks of age (data not shown).

The present study found that *in vivo* [^{3}H]QNB binding in the cerebral cortex was significantly decreased in 8-week-old *vs.* 3-week-old mice, despite an increase in Bmax during development. We previously reported an increase of *in vivo* binding of [^{3}H]QNB in the left striatum of rat brain infused with ibotenic acid 14 days prior to the tracer

experiment. On the other hand, *in vitro* autoradiograms showed significant decreases in [^{3}H]QNB binding in serial slices in the same rat due to decrease in number of binding sites [35]. These findings support our hypothesis, because neural cell death induced by ibotenic acid would alter the microenvironment surrounding muscarinic receptors resulting in a loss of the barrier effect. Further research is required to elucidate the reasons underlying this paradox as well as the observed discrepancies between the *in vivo* binding of [^{3}H]QNB and [^{11}C]NMPB. However, our research has demonstrated that the combined use of these radioligands is valuable for examining the physiological and pharmacological roles of barrier-modulation in the developing brain.

5. Conclusion

A significant discrepancy between the *in vivo* binding of [^{3}H]QNB and [^{11}C]NMPB was observed in the cerebral cortex of mice during the 3 to 8 week period of development. Increased [^{11}C]NMPB binding is most likely due to an increase in Bmax. On the other hand, *in vivo* binding of [^{3}H]QNB in 8-week-old mice was significantly decreased relative to that exhibited by their 3-weeks-old counterparts. Though the reason for the discrepancy between the *in vivo* binding of [^{3}H]QNB and [^{11}C]NMPB remains unclear, we hypothesize that a heightened barrier-effect in the developing brain accounts for

these contradictory observations. Future studies on the effect of membrane lipid components on *in vivo* binding of [^{3}H]QNB are required.

Conflict of Interest

The authors have no conflicts of interest.

Acknowledgments

The authors wish to thank Dr. Rie Hosoi for her kind assistance with *in vitro* [^{3}H]QNB binding experiments

References

[1] Graef S, Schönknecht P, Sabri O, Hegerl U. Cholinergic receptor subtypes and their role in cognition, emotion, and vigilance control: an overview of preclinical and clinical findings. Psychopharmacology (Berl) 2011;215:205-229.

[2] Andersson DR, Björnsson E, Bergquist F, Nissbrandt H. Motor activity-induced dopamine release in the substantia nigra is regulated by muscarinic acetylcholine receptor. Exp Neurol 2010;221:251-259.

[3] Power AE. Muscarinic cholinergic contribution to memory consolidation: with attention to involvement of the basolateral amygdala. Curr Med Chem 2004;11:987-996.

[4] Andersson KE, Campeau L, Olshansky B. Cardiac effects of muscarinic receptor antagonists used for voiding dysfunction. Br J Clin Pharmacol 2011;72:186-196.

[5] Lipworth BJ. Emerging role of long acting muscarinic antagonists for asthma. Br J Clin Phamacol 2014;77:55-62.

[6] Hulme EC, Birdsall NJ, Buckley NJ. Muscarinic receptor subtypes. Annu Rev Pharmacol Toxicol 1990;30:663-673.

[7] Mash DC, Potter LT. Autoradiographic localization of M1 and M2 muscarinic receptors in the rat brain. Neuroscience 1986;19:551-564.

[8] Wang JX, Roseke WR, Gulya K, Wang W, Yamamura HI. [3H]AF-DX 116 labels

subsets of muscarinicreceptors in rat brain and heart. Life Sci. 1987;41:1751-1760.

[9] Yamamura HI, Snyder SH. Muscarinic cholinergic binding in rat brain. Proc Natil Acad Sci U S A 1974;71:1725-1729.

[10] Yamamura HI, Kuhar MJ, Snyder SH. In vivo identification of muscarinic cholinergic receptor binding in rat brain. Brain Res 1974;80:170-176.

[11] Ellis J, Hoss W. Analysis of regional variations in the affinities of muscarinic agonist in the rat brain. Brain Res 1980;193:189-198.

[12] Gilbert PFT, Hanley MR, Iversen LL. [3H]-quinuclidinyl benzylate binding to muscarinic receptors in rat brain : Comparison of results from intact brain slice and homogenate. Br. J. Pharmac 1979; 65:451-454

[13] Kloog Y, Sokolovsky M. Studies on muscarinic acetylcholine receptors from mouse brain: characterization of the interaction with antagonists. Brain Res 1978;144:31-48.

[14] Kloog Y, Egozi Y, Sokolovsky M. Regional heterogeneity of muscarinic receptors of mouse brain. 1979 FEBS Letters;97(2):265-268.

[15] Kloog Y, Egozi Y, Sokolovasky M. Characterization of muscarinic acetylcholine receptorsfrom mouse brain: evidence for regional heterogeneity and internalization. Mol Pharmacol 1979;15:545-558.

[16] Kobayashi RH, Palkovits M, Hruska R, Rothschild R, Yamamura HI.

Regionaldistribution of muscarinic cholinergic receptors in rat brain. Brain Res 1978;154;13-23.

[17] Gilter MS, De La Cruz R, Zeeberg BR, Reba RC. [3H]QNB displays in vivo selectivity for the m2 subtype. Life Sci 1994;55:1493-1508.

[18] Hosoi R, Kobayashi K, Watanabe Y, Inoue O. Evaluation of in vivo binding properties of 3H-NMPB and 3H-QNB in mouse brain. J Neural Transm 1999;106:583-592.

[19] Perry DC, Mullis KB, Oie S, Sadee W. Opiate antagonist receptor binding in vivo: evidence for a new receptor binding model. Brain Res 1980;199:49-61.

[20] Okun IM, Merezhinskaya NV, Rakovich AA, Volkovets TM, Aksentsev SL, Konev SV. Inactivation of muscvarinic acetylcholine receptors in brain synaptic membranes by free fatty acids. Evaluation of the role of lipid phase. Gen Physiol Biophys 1986;5:243-258.

[21] Miller LG, Greenblatt DJ, Roy RB, Lopez F, Wecker L. Dietary choline intake modulates benzodiazepine receptor binding and gannma-aminobutyric acidA receptor function in mouse brain. J Pharmacol Exp Ther 1989;248(1):1-6.

[22] Giménez R, Raïch J, Aguilar J. Changes in brain striatum dopamine and acetylcholine receptors induced by chronic CDP-choline treatment of aging mice. Br J

Pharmacol 1991;194:575-578.

[23] Berstein G, Haga T, Ichiyama A. Effect of the lipid environment on the differential affinity of purified cerebral and atrial muscarinic acetylcholine receptors for pirenzepine. Mol Pharmacol 1989;36:601-607.

[24] Ghosh C, Dick RM, Ali SF. Iron/ascorbate-induced lipid peroxidation changes membrane fluidity and muscarinic cholinergic receptor binding in rat frontal cortex. Neurochem Int 1993;23:479-484.

[25] Heron DS, Shinitzky M, Hershkowitz M, Samuel D. Lipid fluidity markedly modulate the binding of serotonin to mouse brain membrane. Proc Natl Acad Sci USA 1980;77:7463-7467.

[26] Suzuki K, Inoue O, Hashimoto K, Yamasaki T, Kuchiki M, Tamate K. Computer-controlled large scale production of high specific activity [11C]RO 15 1788 for PET studies of benzodiazepine receptors. Int J Appl Radiat Isot 1985;36:971-976.

[27] Patlak CS, Blasberg RG, Fenstermacher JD. Graphical evaluation of blood-to-brain transfer constants from multiple-time uptake data. J Cereb Blood Flow Metab 1983;3:1-7.

[28] Aronstam RS, Kellogg C, Abood LG. Development of muscarinic cholinergic receptors in inbred strains of mice: identification of receptor heterogeneity and relation

to audiogenic seizer susceptibility. Brain Res 1979;162:231-241.

[29] Wei JW, Hung WC. Differential distribution of muscarinic receptor subtypes and their regulation by G-protein in rat brain. Gen .Pharmac 1990;21(4):471-476

[30] Bakker G, Vingerhoets WA, van Wieringen JP, de Bruin K, Eersels P, de Jong J, Chahid Y, Rutten BP, DuBois S, Watson M, Mogg AJ, Xiao H, Crabtree M, Collier DA, Felder CC, Barth VN, Broad LM, Bloemen OJ, van Amelsvoort TA, Booij J. 123I-iododexetimide preferentially binds to the muscarinic receptor subtype M1 in vivo. J Nucl Med 2015;56(2):317-322.

[31] Jagoda EM, Kiesewetter DO, Shimoji K, Ravasi I, Yamada M, Gomeza J, Wess J, Eckelman WC. Reigional brain uptake of the muscarinic ligand, [18F]FP-TZTP, is greatly decreased in M2 receptor Knockout mice but not in M1,M3and M4receptor knockout mice. Neuropharmacology. 2003;44:653-661.

[32] McRee RC, Boulay SF, Sood VK, Cohen VI, Gilter MS,Zeeberg BR, Gibson RE, Reba RC. Autoradiographic evidence that QNB displays in vivo selectivity for the m2 subtype. Neuroimage 1995;2:55-62.

[33] Sadee W, Perry DC, Rosenbaum JS, Herz A. [3H]diprenorphine receptor binding in vivo and in vitro. Eur J Pharmacol 1982;81:431-440.

[34] Inoue O, Kobayashi K, Gee A. Changes in apparent rates of receptor binding in the

intact brain in relation to the heterogeneity of reaction environments. Crit Rev Neurobiol 1999;13:199-225.

[35] Nakano T, Yanamoto K, Amitani M, Momosaki S, Hosoi R, Inoue O. Radioisotores 2006;55:29-33. DOI:https://doi.org/10.3769/radioisotopes.55.29

Tables

Table 1. In vitro binding parameters of [^{3}H]QNB in the cerebral cortex of 3- and 8-week-old mice. Values are represented as mean ± SD of five runs for cereberal cortex of 3- and 8-week-old mice, three runs for cerebellum of 3-week-old mice, and four runs for cerebellum of 8-week-old mice. * p<0.01; 3-week-old mice vs. 8-week-old mice.

	Cerebral Cortex		Cerebellum	
	K_d	B_{max}	K_d	B_{max}
3 weeks	0.110 ± 0.017	0.159 ± 0.015	0.050 ± 0.022	0.019 ± 0.003
8 weeks	0.102 ± 0.020	0.195 ± 0.018*	0.056 ± 0.022	0.016 ± 0.003

Table 2. The time course of radioactivity concentration in the plasma, cerebral cortex, and cerebellum following injection of [^{3}H]QNB with (CA) or without (CF) 3 mg/kg of carrier QNB into 3-week-old mice. Values are expressed as percent injected dose / gram tissue or mean ± SD of the three mice in each group.

Time (min)	Absence of carrier QNB (CF)		
	Plasma	Cerebral Cortex	Cerebellum
1	2.52 ± 0.14	6.39 ± 0.33	5.85 ± 0.53
5	4.05 ± 0.19	10.0 ± 1.1	7.82 ± 0.45
10	5.14 ± 0.45	12.8 ± 0.3	8.46 ± 0.41
20	5.19 ± 0.37	14.2 ± 0.5	8.53 ± 0.86
30	4.73 ± 0.25	14.9 ± 0.8	8.55 ± 0.61
45	3.47 ± 0.05	17.1 ± 0.6	9.34 ± 0.25
60	2.82 ± 0.37	16.7 ± 0.6	8.95 ± 1.15

Time (min)	Presence of carrier QNB (CA)		
	Plasma	Cerebral Cortex	Cerebellum
1	2.36 ± 0.11	6.66 ± 0.73	6.01 ± 0.21
5	3.48 ± 0.13	8.13 ± 0.31	6.87 ± 0.19
10	5.18 ± 0.41	6.24 ± 0.25	4.91 ± 0.17
20	5.74 ± 0.07	4.47 ± 0.26	3.40 ± 0.32
30	5.10 ± 0.20	2.44 ± 0.25	1.67 ± 0.15
45	3.76 ± 1.11	1.67 ± 0.16	1.19 ± 0.09
60	2.99 ± 0.37	1.13 ± 0.16	0.79 ± 0.08

Table 3. The time courses of radioactivity concentration in the plasma, cerebral cortex, and cerebellum following injection of [^{11}C]NMPB with (CA) or without (CF) 3 mg/kg of carrier QNB into 3-week-old mice. Values are expressed as percent injected dose / gram tissue or mean ± SD of the three mice in each group.

Time (min)	Absence of carrier QNB (CF)		
	Plasma	Cerebral Cortex	Cerebellum
1	2.54 ± 0.08	15.1 ± 2.0	11.2 ± 1.0
5	3.39 ± 0.24	21.9 ± 2.6	12.1 ± 0.8
10	3.63 ± 0.30	25.7 ± 1.7	10.2 ± 1.0
20	3.52 ± 0.31	24.8 ± 1.6	5.55 ± 0.46
30	3.36 ± 0.18	24.2 ± 2.1	3.56 ± 0.55
45	2.46 ± 0.14	22.5 ± 1.9	2.47 ± 0.22
60	2.31 ± 0.45	20.3 ± 1.5	1.67 ± 0.20

Time (min)	3mg/kg carrier QNB (CA)		
	Plasma	Cerebral Cortex	Cerebellum
1	2.41 ± 0.11	13.0 ± 1.5	11.2 ± 0.6
5	2.64 ± 0.04	14.7 ± 0.1	12.6 ± 0.2
10	3.20 ± 0.17	11.9 ± 0.4	9.10 ± 0.38
20	3.52 ± 0.22	7.92 ± 1.79	5.99 ± 1.27
30	3.71 ± 0.17	3.99 ± 0.16	3.11 ± 0.12
45	2.85 ± 0.75	2.29 ± 0.39	1.95 ± 0.29
60	2.46 ± 0.23	1.39 ± 0.17	1.21 ± 0.13

Table 4. The time course of radioactivity concentration in the plasma, cerebral cortex, and cerebellum following injection of [^{3}H]QNB with (CA) or without (CF) 3 mg/kg of carrier QNB into 8-week-old mice. Values are expressed as percent injected dose / gram tissue or mean ± SD of the three mice in each group.

Time (min)	Absence of carrier QNB (CF)		
	Plasma	Cerebral Cortex	Cerebellum
1	1.19 ± 0.07	1.83 ± 0.19	1.51 ± 0.06
5	1.42 ± 0.26	2.41 ± 0.16	1.87 ± 0.07
10	1.64 ± 0.03	2.95 ± 0.03	2.11 ± 0.07
20	1.73 ± 0.11	3.61 ± 0.08	2.49 ± 0.14
30	1.39 ± 0.02	3.84 ± 0.08	2.58 ± 0.05
45	1.30 ± 0.13	4.05 ± 0.21	2.81 ± 0.15
60	0.93 ± 0.11	4.40 ± 0.11	2.83 ± 0.09

Time (min)	3mg/kg carrier QNB (CA)		
	Plasma	Cerebral Cortex	Cerebellum
1	1.12 ± 0.06	2.51 ± 0.28	2.33 ± 0.16
5	1.31 ± 0.05	2.36 ± 0.28	2.00 ± 0.27
10	1.30 ± 0.10	1.83 ± 0.21	1.46 ± 0.18
20	1.84 ± 0.04	1.44 ± 0.12	0.96 ± 0.07
30	1.62 ± 0.08	0.91 ± 0.14	0.58 ± 0.11
45	1.31 ± 0.06	0.60 ± 0.06	0.46 ± 0.04
60	1.02 ± 0.07	0.51 ± 0.02	0.39 ± 0.03

Table 5. The time course of radioactivity concentration in the plasma, cerebral cortex, cerebellum, and heart following injection of [^{11}C]NMPB with (CA) or without (CF) 3 mg/kg of carrier QNB into 8-week-old mice. Values are expressed as percent injected dose / gram tissue or mean ± SD of the three mice in each group.

Time (min)	Absence of carrier QNB (CF)		
	Plasma	Cerebral Cortex	Cerebellum
1	1.30 ± 0.13	6.78 ± 0.34	4.96 ± 0.31
5	1.24 ± 0.21	9.61 ± 0.51	5.57 ± 0.13
10	1.40 ± 0.04	11.4 ± 0.5	4.48 ± 0.32
20	1.42 ± 0.05	13.5 ± 0.2	3.02 ± 0.21
30	1.05 ± 0.05	13.3 ± 0.2	1.80 ± 0.10
45	1.07 ± 0.22	13.3 ± 0.9	1.41 ± 0.25
60	0.73 ± 0.11	13.4 ± 0.9	1.00 ± 0.17

Time (min)	3 mg/kg carrier QNB (CA)		
	Plasma	Cerebral Cortex	Cerebellum
1	1.15 ± 0.07	5.71 ± 0.60	4.87 ± 0.38
5	1.11 ± 0.05	5.98 ± 0.78	4.79 ± 0.63
10	1.23 ± 0.13	4.40 ± 0.53	3.43 ± 0.44
20	1.41 ± 0.06	2.99 ± 0.31	2.14 ± 0.23
30	1.28 ± 0.06	1.79 ± 0.25	1.24 ± 0.20
45	1.05 ± 0.14	0.97 ± 0.11	0.70 ± 0.08
60	0.80 ± 0.11	0.61 ± 0.04	0.46 ± 0.05

Table 6. In vivo saturation of [^{3}H]QNB binding in the cerebral cortex and cerebellum of 3-week-old mice. Values are expressed as percent injected dose / gram tissue or mean ± SD of the three mice in each group.

Dose (μg/kg) *	Cerebral Cortex	Cerebellum
0	13.13 ± 1.31	8.45 ± 0.64
10	12.50 ± 0.73	4.32 ± 0.17
30	12.39 ± 1.05	2.60 ± 0.28
100	6.18 ± 0.23	1.87 ± 0.26
300	3.08 ± 0.20	1.57 ± 0.14
1000	1.78 ± 0.12	1.37 ± 0.02
3000	1.28 ± 0.13	1.13 ± 0.13

*Doses of carrier QNB

Legends for Figures

Figure 1

Patlak plot for the [^{3}H]QNB binding in the cerebral cortex and cerebellum in 3- and 8-week-old mice. Free-ligand concentrations were assumed to correspond to the non-specific binding at each time point. CF: radioactivity concentration in the cerebral cortex and cerebellum at each time point after the injection of [^{3}H]QNB into 3- and 8week old mice. CA: radioactivity concentration in the cerebellum at each time point after the injection of [^{3}H]QNB with 3 mg/kg of carrier QNB into 3w or 8 week old mice. The average of the ratio of radioactivity concentration (CF/CA) at each time point was used. Normalized integral time was calculated as follows; Σ CA/CA. Statistical analysis was performed for the slope of regression line for the cerebral cortex and cerebellum between 3w and 8 weeks old mice. Sttistical significance ($p<0.01$) was observed in the slope of regression line for the cerebral cortex.

Figure 2

Patlak plot for the [^{11}C]NMPB binding in the cerebral cortex and cerebellum in 3- and 8-week old mice. Free ligand concentrations were assumed to correspond to the non-specific binding at each time point. CF: radioactivity concentration in the cerebral

cortex and cerebellum at each time point after the injection of [^{11}C]NMPB into 3- and 8week old mice. CA: radioactivity concentration in the cerebellum at each time point after the injection of [^{11}C]NMPB with 3 mg/kg of carrier QNB into 3- and 8 week old mice. The average of the ratio of radioactivity concentration (CF/CA) at each time point was used. Normalized integral time was calculated as follows; Σ CA/CA. Statistical analysis was performed for the slope of regression line for the cerebral cortex and cerebellum between 3- and 8 week old mice. Sttistical significance ($p<0.01$) was observed in the slope of regression line for the cerebral cortex.

Figure 3

Scatchard plot for *in vivo* binding of [^{3}H]QNB in the cerebral cortex and cerebellum of 3-week-old mice. The specific binding in the cerebellum was assumed to be saturated by 300 μg/kg of carrier QNB.

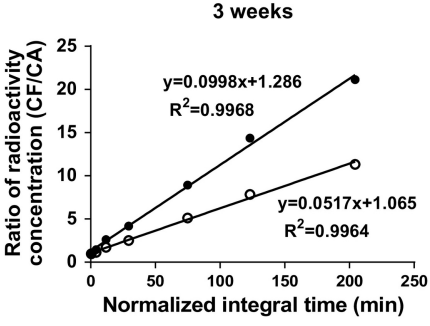

estimated k3
Cerebral Cortex: 0.0998 min^{-1}
Cerebellum: 0.0517 min^{-1}

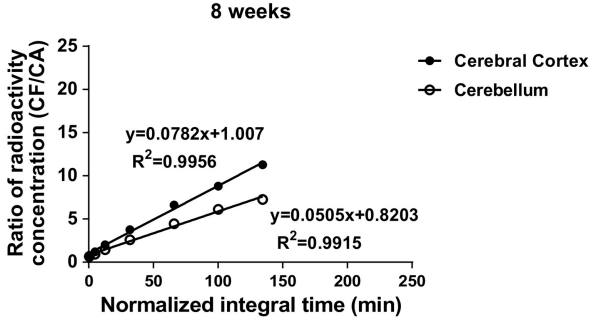

estimated k3
Cerebral Cortex: 0.0782 min^{-1}
Cerebellum: 0.0505 min^{-1}

Figure 1

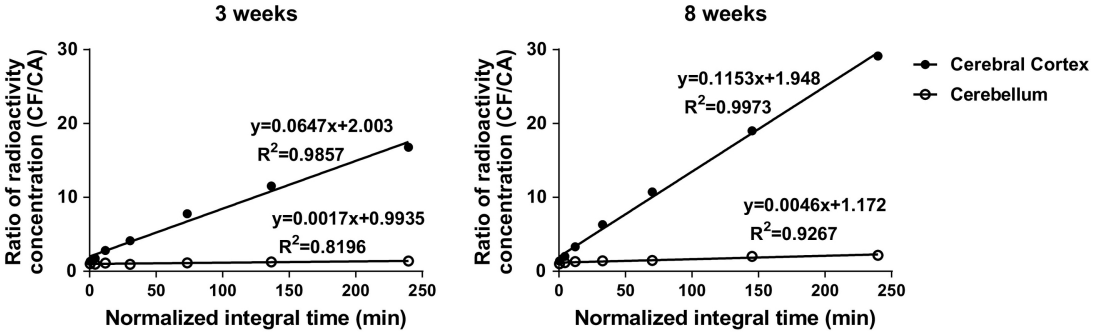

estimated k3
Cerebral Cortex: 0.0647 min^{-1}
Cerebellum: 0.0017 min^{-1}

estimated k3
Cerebral Cortex: 0.1153 min^{-1}
Cerebellum: 0.0046 min^{-1}

Figure 2

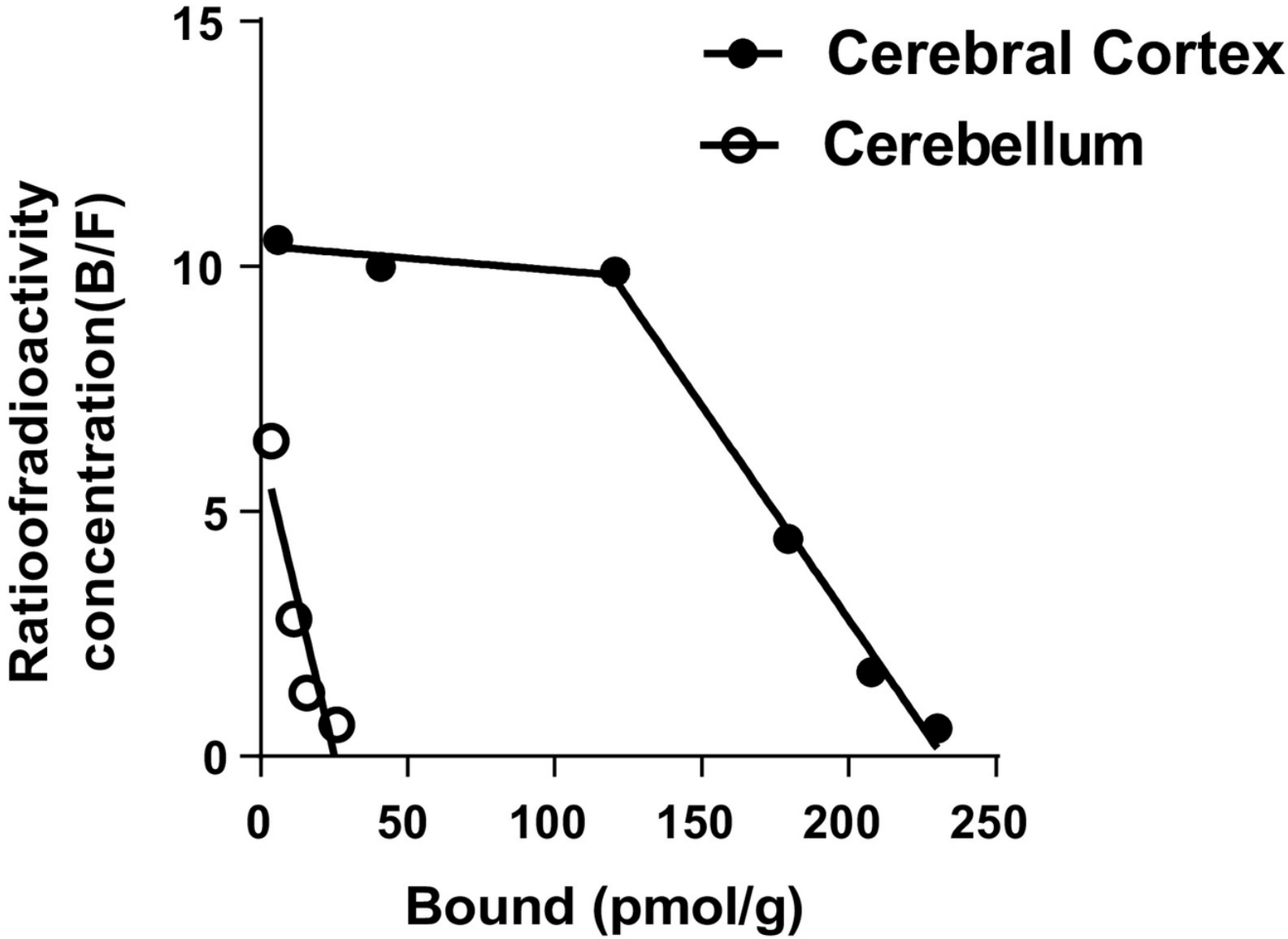
Cerebral Cortex
Cerebellum
Ratioofradioactivity concentration(B/F)
15
10
5
0
0
50
100
150
200
250
Bound (pmol/g)

Figure 3